

MEASUREMENT OF DYNAMIC STATE OF LANDSLIDE DISASTER

Kosuke Tande, Shotaro Niimi, and Shigeru Takayama

Department of Electrical & Electronic Engineering, Science & engineering
Ritsumeikan University, BKC, Shiga, Japan, re006073@ed.ritsumei.ac.jp

Abstract: Sensing node network system (SNNS) is a compatible system for monitoring landslide disaster. Sensing node consists of sensors, data processing unit and wireless communication unit. In detection of landslide occurrence and grasping posture of sensing node; acceleration sensor is use. This paper describes the observation and estimation method of dynamic spatial behaviour of sensing node by acceleration signal. By monitoring the dynamic situation of the angles between acceleration vectors in three orthogonal axes, the posture and dynamic behaviour of sensing node during landslide disaster is estimated.

Keywords: Sensing, Network, Acceleration, Landslide

1. INTRODUCTION

Natural disaster cause massive losses to human beings, culture, economics, and so on. There are many factors which seem lead to the occurrence of landslide in Japan. So it is very important to monitor such danger factors. And if human predict the times and know the factor of landslide, landslide prevention work can be done and mitigate the damages by refuge.

In this paper propose Sensing Node Network System that monitoring landslides, and a method that observing and judging landslide occurrence and dynamic behaviour of sensing node at landslide. Acceleration sensor can measure the gravity, so it is useful for observing static position and dynamic behaviour of sensing node.

2. SENSING NODE NETWORK SYSTEM

This system consists of Local Sensing Node Network System (LSNNS) and Host System. LSNNS consists of Host Node and Sensing Nodes. Sensing node practices autonomous sending measurement data, creating communication routes, and control sampling time. Host node sends data which collected from sensing nodes to host system and sends orders from host system to sensing nodes. LSNNS have the ad hoc network by Specified Low Power Radio (SLPR), enable an efficient information gathering of LSNNS and the structure of the system that considers the damage of sensing nodes due to landslide. Host system monitors condition of nodes on the PC.

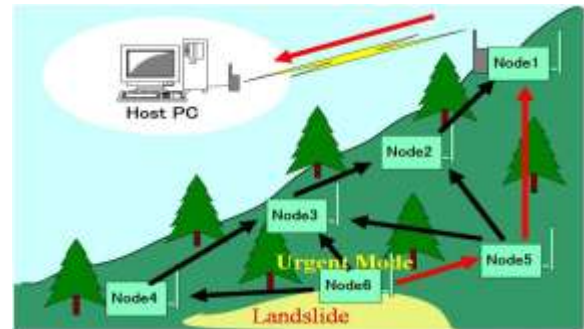


Fig.1 SNNS

A sensing node consists of sensor units, GPS unit, wireless communication unit, control board, and power supply. As for sensor unit, acceleration sensor and temperature sensor is being use. SLPR equipment is use as wireless communication unit, battery as power supply, and AP - SH3D - 1A as control board.

3. ACCELERATION SENSOR

Fig.2 shows acceleration sensor (KXM52 - 1050) installed in sensing node. (The voltage is [3.3V])

- 1) Acceleration Range $\pm 2[G]$
- 2) Sensitivity 660[mV]
- 3) Offset Voltage 165[V]
- 4) Supply Voltage 2.7[V] to 5.5[V] VDC

*KXM52 - 1050 has the offset voltage error maximum $\pm 167[mV]=\pm 0.253[G]$ and sensitivity error $\pm 5\%$.

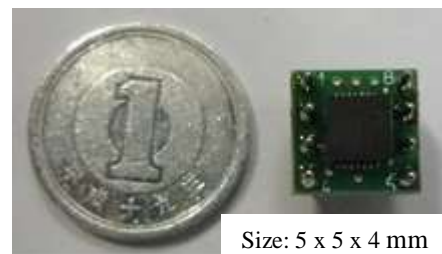


Fig.2 KXM52 - 1050

4. MONITORING OF LANDSLIDE BY ACCELERATION INFORMATION

When the acceleration sensor reacts vibrations, the sensing node starts measuring acceleration data. But the acceleration sensor reacts various effects (conflict, moving and so on). So, it is necessary to distinguish landslide and not landslide from acceleration data.

In addition to this, landslide has some pattern. In this paper, "Slide Down" means sensing node slip down with the surface of the slope, "Rolling Down" means sensing node involved cliff failure. The range and damage are different in these patterns. So, it is important to distinguish landslide pattern.

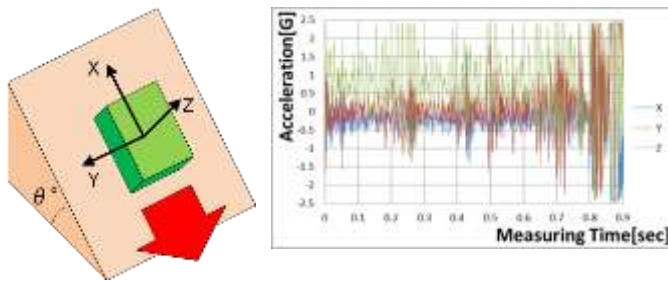


Fig.3 Acceleration data at Landslide

Fig.3 shows acceleration data at Landslide. Due to noise, it is difficult to for further data analysis. So, it is necessary to convert acceleration data.

4.1 Power Spectrum

To calculate power spectrum from Fast Fourier Transform in a short interval.

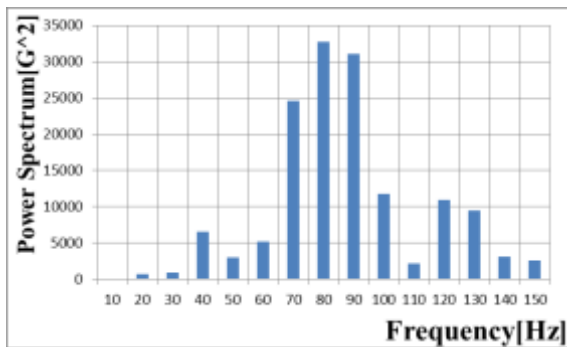


Fig.4 Power Spectrum of Fig.3 in 0.1~0.2[sec]

Fig.4 shows power spectrum of Fig.3 in 0.1~0.2[sec].

4.2 Triaxial Angle

All acceleration data is computed into angles between acceleration vectors in three orthogonal axes (Triaxial angle) as shown in Fig.4

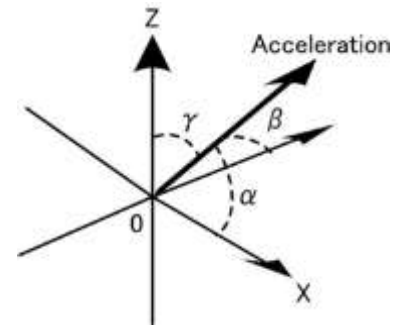


Fig.5 Triaxial angle

Acceleration data is computed to angles using Eq. (1).

$$\begin{aligned} \alpha[\text{deg}] &= \arccos(x/|A|) * 180 / \pi \\ \beta[\text{deg}] &= \arccos(y/|A|) * 180 / \pi \\ \gamma[\text{deg}] &= \arccos(z/|A|) * 180 / \pi \end{aligned} \quad (1)$$

x, y, z value are average of acceleration data[G] for every 1024 data. A is acceleration vector computed from x, y, z value.

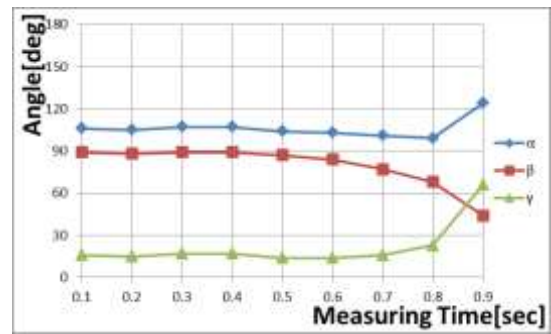


Fig.6 Triaxial angle of Fig.3

In that way, it is easier to judge sensing node's position. By using the angle value and acceleration vector; enable node condition judgment.

5. DETECTION OF LANDSLIDE OCCURRENCE

To detect landslide occurrence by Power Spectrum and Triaxial Angle. Fig.7 shows the flowchart of the detection.

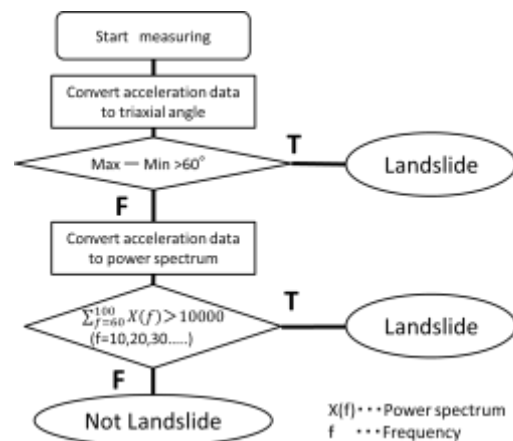


Fig.7 Flowchart of detecting landslide occurrence

The sensing node detects landslide occurrence by this flowchart.

5.1 Experiment of not landslide (Collision)

Fig.8 shows the experiment of not landslide (Collision), and Fig.8 shows the result.

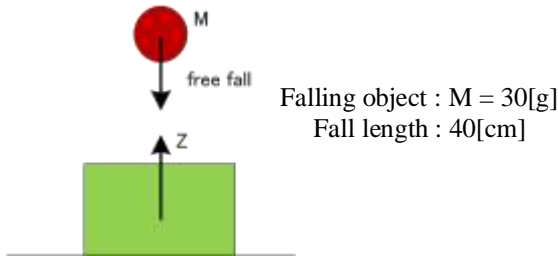


Fig.8 Experiment of not landslide (Collision)

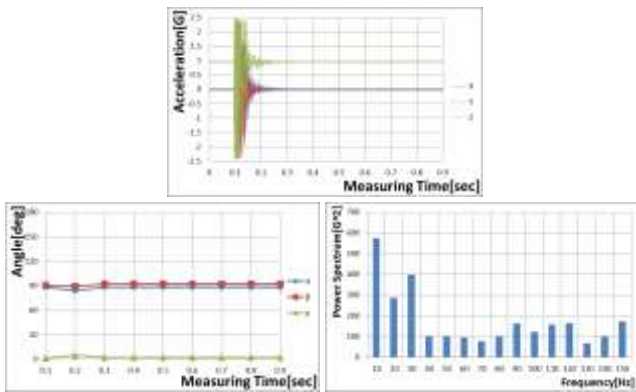


Fig.9 Acceleration, angle and power spectrum at not landslide (Collision)

According to Fig.9, (max_triangular angle – min_triangular angle) is less than 60, and $\Sigma X(f)$ is less than 10000. So, this case is detected not landslide.

5.2 Experiment of landslide (Slide Down)

Fig.10 shows the experiment of landslide (Slide Down), and Fig.10 shows the result.



Slope length : 4[m]
Tilt angle : 35[deg]

Fig.10 Experiment of landslide (Slide Down)

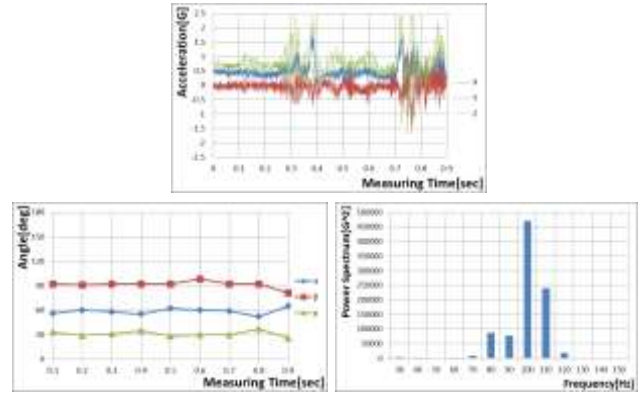


Fig.11 Acceleration, angle and power spectrum at not landslide (Slide Down)

In “Slide Down”, the sensing node slips down with keeping position. So, the change of triaxial angle is little.

According to Fig.11, (max_triangular angle – min_triangular angle) is less than 60, and $\Sigma X(f)$ is over than 10000. So, this case is detected landslide.

5.3 Experiment of landslide (Rolling Down)

Fig.12 shows the experiment of landslide (Rolling Down), and Fig.13 shows the result.



Slope length : 4[m]
Tilt angle : 35[deg]

Fig.12 Experiment of landslide (Rolling Down)

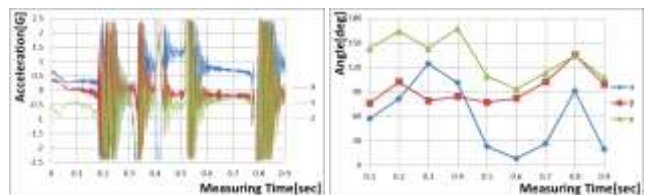


Fig.13 Acceleration and angle at landslide (Rolling Down)

In “Rolling Down”, the sensing node fall down with changing position. So, the change of triaxial angle is big.

According to Fig.13, (max_triangular angle – min_triangular angle) is over than 60. So, this case is detected landslide.

6. ESTIMATION OF LANDSLIDE PATTERN

The method of determining landslide pattern is computed as below. All of 9 data of three angles α , β and γ are use in 3 important steps from (a) ~ (c).

(a) First, maximum and minimum of three angles α , β and γ are selected from 9 data, and the value of dec(I) is computed by using Eq. (2).

$$\begin{aligned} PP1 < 5 & : dec(I) = 0 \\ 5 \leq PP1 < 60 & : dec(I) = 1 \\ 60 \leq PP1 & : dec(I) = 2 \end{aligned} \quad (2)$$

* PP1 : (maximum) - (minimum)
dec(I) : Fragment

(b) Second, maximum and minimum of three angles α , β and γ are removed from the data.

(c) Third, maximum and minimum of three angles α , β and γ are selected from 7 data left, and the value of dec(II) is computed by using Eq. (3)

$$\begin{aligned} PP2 < 5 & : dec(II) = 0 \\ 5 \leq PP2 < 30 & : dec(II) = 1 \\ 30 \leq PP2 & : dec(II) = 2 \end{aligned} \quad (3)$$

* PP2 : (maximum) - (minimum)
dec(II) : Fragment

The maximum data of dec(I), dec(II) are use as max_dec(I) and max_dec(II). max_dec(I) and max_dec(II) value are use to observe the change of the angle transition. Table 1 shows the judgment standard using the angle data.

Table 1 Judgment standard for angle data

max_dec(I)	max_dec(II)	Landslide pattern
0	0	Collision
1	0	Collision
1	1	Slide Down
2	1	Slide Down
2	2	Rolling Down

The angle data of Fig.9, Fig.11 and Fig.13 are shows in Table2, Table3 and Table4 according to this judgment method.

Table 2 Judgment of data for Fig.8

Step		MAX	MIN	PP	dec	Max_dec
(a)	α	88	84	4	0	0
	β	92	89	3	0	
	γ	5	1	4	0	
(c)	α	88	88	0	0	0
	β	90	90	0	0	
	γ	2	2	0	0	

Table 1 shows that Fig.9 is "Collision" as Table 2 shows that max_dec(I) and max_dec(II) is 0.

Table 3 Judgment of data for Fig.10

Step		MAX	MIN	PP	dec	Max_dec
(a)	α	65	52	13	1	1
	β	98	81	17	1	
	γ	37	26	11	1	
(c)	α	62	55	7	1	1
	β	92	91	1	0	
	γ	35	28	7	1	

Table 1 shows that Fig.11 is "Slide Down" as Table 3 shows that max_dec(I) and max_dec(II) is 1.

Table 4 Judgment of data for Fig.12

Step		MAX	MIN	PP	dec	Max_dec
(a)	α	124	8	116	2	2
	β	135	76	59	2	
	γ	167	93	74	2	
(c)	α	101	19	82	2	2
	β	102	77	25	1	
	γ	164	107	57	2	

Table 1 shows that Fig.13 is "Rolling Down" as Table 4 shows that max_dec(I) and max_dec(II) is 2.

7. ESTIMATION OF THE STRENGTH OF LANDSLIDE

The strength of landslide is proportional to the energy added to the sensing node. So if kinetic energy of the sensing node becomes clear, intercomparison of the strength of landslide becomes possible.

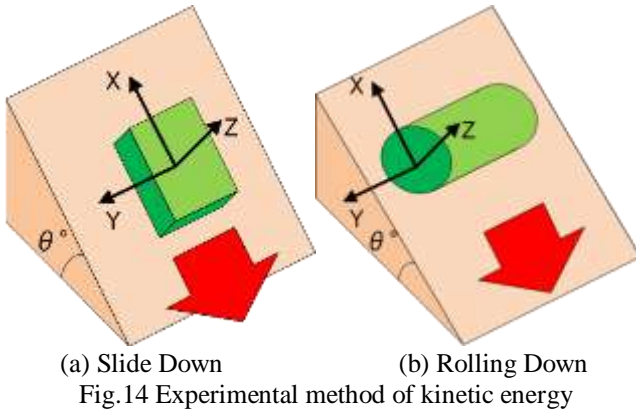
$$\begin{cases} E = \frac{1}{2}mv^2 \\ v = \int_0^T \alpha dt = \sum_{n=1}^N \alpha_n + v_0 \end{cases} \quad (4)$$

*E : kinetic energy
 m : mass of sensing node
 v : velocity of sensing node
 T : measuring time
 α : acceleration
 v₀ : initial velocity

Eq. (4) is a formula for kinetic energy.
 If “m” and “T” are constant, then Eq. (5) is approved by Eq. (4).

$$E \propto \left(\sum_{n=1}^N \alpha_n + v_0 \right)^2 \quad (5)$$

So, the strength of landslide is estimated from acceleration.
 For verification of Eq. (5), slide and rolling down a sensing node on the slope like Fig. 14.



While tilt angle is bigger, the energy added to the sensing node is bigger too. In this experiment, θ is changed 15[deg] to 30[deg] per 5[deg]. The result is shown below. The kinetic energy is calculated from Eq. (6).

$$E = \frac{1}{2} m \left(\sum_{n=0}^{n_0+N-1} \alpha_n + v_0 \right)^2 \quad (6)$$

7.1 Experiment of Slide Down

In experiment of Slide Down, use the first 0.1 second acceleration data from beginning to slide. Kinetic energy is calculated from Eq. (6) as m=1, v₀=0, n₀=1, N=1024.

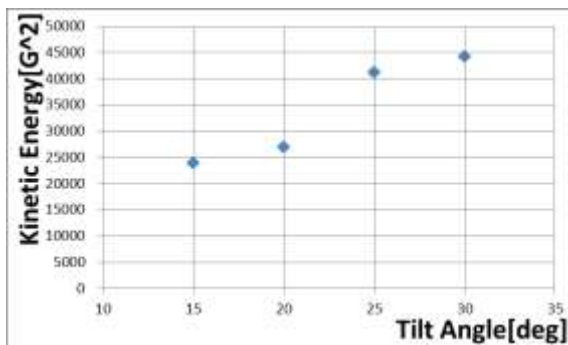


Fig.15 Change of kinetic energy due to tilt angle

Fig.15 shows change of kinetic energy due to tilt angle. According to Fig.15, the kinetic energy is proportional to the tilt angle. Therefore it is likely to say that the strength of Slide Down and the kinetic energy are proportional relativity.

7.2 Experiment of Rolling Down

In experiment of Rolling Down, use the average of every 200 acceleration data from beginning. Kinetic energy is calculated from Eq. (6) as m=1, v₀=0, N=200.

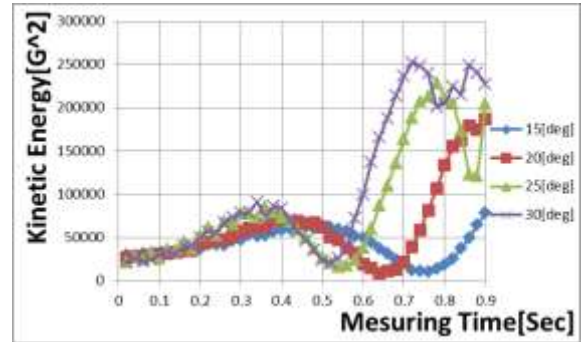


Fig.16 Change of kinetic energy of each tilt angle

Fig.16 shows change of kinetic energy of each tilt angle. According to Fig.16, the bigger tilt angle, the bigger magnitude of the peak. The bigger tilt angle is, the earlier the bottom appears. By these characteristic, it is likely to say that the strength of Rolling Down can be compared relatively.

8. CONCLUSIONS

According to the study, landslide occurrence can be distinguished by triaxial angle and power spectrum. The landslide pattern can be estimated by change of triaxial angle. The strength of landslide can be estimated by kinetic energy. For further study, several experiments with difference condition have to be executed in measurement of standard threshold for every judgment. Experiment on real field also needs to be executed for evaluation of current system landslide distinguishes performance.

9. REFERENCES

- [1] H.Soeda, “Application of Telemetry to Aquatic Animal Behavior”, Kouseisya kouseikaku, (1990)
- [2] Information - Communication System of Disasters Prevention Association, “Information - Communication System of Disasters Prevention”, Sankaido, pp.1 - 73 (2003)
- [3] Kyoto University Disasters Prevention laboratory, “Foundation Disaster”, Sankaido, pp.9 - 21 (2003)
- [4] A.Takei, “Landslide,collapse,mudslide - Prediction and Measure -”, Kashima publishing, pp.65 - 77 (1980)
- [5] T.Nagata, “Robot system that aim at autonomous decentralizaion”, Ohmsha

- [6] K.Ikeda, "Some Aspects of New Biotelemetry System", Japanese Journal of Medical Electrons and Biological Engineering, Vol.18, No.7, pp.479 - 484 (1980)
- [7] H.Kadono, "Application of Biotelemetry for Ecology", Japanese Journal of Medical Electrons and Biological Engineering, Vol.18, No.7, pp.485 - 491 (1980)
- [8] K.Shimizu, "Optical Biotelemetry", Japanese Journal of Medical Electrons and Biological Engineering", Vol.18, No.7, pp.492 - 498 (1980)
- [9] I.Matsuzawa, "Natural Disasters Science Subject - book", Tsukijisyokan(1991)
- [10] I.Ishii, "Disaster Prevention engineering", Morikita publishing(1996)
- [11] Trimpe, S.; D'Andrea, R.; , "Accelerometer-based tilt estimation of a rigid body with only rotational degrees of freedom," Robotics and Automation (ICRA), 2010 IEEE International Conference on , vol., no., pp.2630-2636, 3-7 May 2010
- [12] Čech, P.; Dlouhý, J.; Čížek, M.; Vícha, I.; Rozman, J.; , "Head position monitoring system design," Radioelektronika (RADIOELEKTRONIKA), 2010 20th International Conference , vol., no., pp.1-4, 19-21 April 2010
- [13] Qian, J.; Fang, B.; Yang, W.; Luan, X.; Nan, H.; , "Accurate Tilt Sensing with Linear Model," Sensors Journal, IEEE , vol.PP, no.99, pp.1, 0